PTEP

Prog. Theor. Exp. Phys. **2023** 103H02(8 pages)
DOI: 10.1093/ptep/ptad124

Kinetic inductance detectors on calcium fluoride substrate for astroparticle physics

K. Ishidoshiro [1,2,⋆], T. Kobayashi[3], K. Hosokawa [4], Y. Kawamura[3], Y. Kamei [1,5], S. Mima [5,6], C. Otani[7,8], A. A. Suzuki[1], M. Zulfakri[9], and T. Taino[3]

[1] *Research Center for Neutrino Science, Tohoku University, 6-3 Aoba, Aramaki, Aoka-ku, Sendai, Miyagi 980-8578, Japan*
[2] *International Center for Quantum-field Measurement Systems for Studies of the Universe and Particles (QUP, WPI), High Energy Accelerator Research Organization (KEK), 1-1 Oho, Tsukuba, Ibaraki 305-0801, Japan*
[3] *Graduate School of Science and Engineering, Saitama University, 255 Shimo Okubo, Sakura-ku, Saitama 338-8570, Japan*
[4] *Kamioka Observatory, Institute for Cosmic-Ray Research, The University of Tokyo, 456 Higashi-Mozumi, Kamioka, Hida, Gifu 506-1205, Japan*
[5] *Center for Advanced Photonics, RIKEN, 2-1 Hirosawa, Wako, Saitama, 351-0798, Japan*
[6] *Advanced ICT Research Institute, National Institute of Information and Communications Technology, Kobe 651-2492, Japan*
[7] *Center for Advanced Photonics, RIKEN, 519-1399 Aoba, Aramaki, Aoba-ku, Sendai, Miyagi 980-0845, Japan*
[8] *Department of Physics, Tohoku University, 6-3 Aoba, Aramaki, Aoka-ku, Sendai, Miyagi 980-8578, Japan*
[9] *School of Electrical Engineering, College of Engineering, Universiti Teknologi MARA, Shah Alam, Selangor 40450, Malaysia*
⋆E-mail: koji@awa.tohoku.ac.jp

Received May 14, 2023; Revised September 18, 2023; Accepted September 22, 2023; Published October 6, 2023

We propose the utilization of inorganic crystals as substrates for kinetic inductance detectors (KIDs), which are thin-film superconducting resonators, for future rare event studies. When energy is deposited on the substrate, phonons are generated and propagate from the substrate to the surface, where KIDs are fabricated. This approach expands the potential for utilizing a diverse range of target crystals. We implement KIDs on calcium fluoride (CaF_2) substrates, since ^{19}F is sensitive to dark matter with spin-dependent interaction and ^{48}Ca is one of the double-β decay nuclei. We have experimentally demonstrated the operation of the KIDs on the CaF_2 substrate and their phonon-mediated particle detection.

Subject Index H20

1. Introduction

The quest to discover rare events such as dark matter and neutrinoless double beta ($0\nu\beta\beta$) decay in underground laboratories represents a significant frontier in astroparticle physics. In the next generation of experiments, detectors with lower energy thresholds and/or higher energy resolution are required. Lowering the energy threshold of detectors enables us to search for lower-mass dark matter [1]. Enhancing the energy resolution of detectors increases their sensitivity to $0\nu\beta\beta$ decay by diminishing the contamination from normal double beta decay [2]. One of the most promising approaches is the use of superconducting detectors. Several experiments have already utilized the Transition Edge Sensor (TES) [3,4]. Moreover, a pilot study on

the utilization of metallic-magnetic calorimeters (MMCs) is underway [5]. Light dark matter searches using superconducting nanowires have already been demonstrated [6].

Among the various superconducting detectors, the kinetic inductance detector (KID) is a highly attractive option. A KID is composed of a feedline and LC resonators made of superconducting films. The kinetic inductance of superconducting films is dependent on the number of Cooper pairs, and when some energy is absorbed in the films, the Cooper pairs are broken, leading to a change in the kinetic inductance, which in turn alters the resonant frequency. The transmitted voltage of a KID at the resonant frequency is highly sensitive to the absorbed energy. KIDs can be designed with different resonant frequencies, making them highly multiplexable, which is essential for reducing wiring complexity and heat load. Consequently, KID is a promising technique for constructing large detector arrays.

The original KID's maximum sensitive area is only a few mm^2 [7]. To increase this area, a phonon-mediated approach with lumped-element KID (LEKID) was proposed [8] and has been successfully tested [9,10]. Phonons generated by energy deposition on the substrate are transferred to the LEKID which is fabricated on the surface, breaking the Cooper pairs in the LEKID. This phonon-mediated approach has enabled the development of large photon sensors. For example, the CALDER collaboration, which is developing large sensors for highly sensitive $0\nu\beta\beta$ decay searches [11], achieved a baseline resolution of 34 eV root mean square (RMS) with a sensitive area of 5 cm $\times$ 5 cm [12]. The simultaneous measurement of photons and phonons from a Li_2MoO_4 crystal has also been demonstrated [13].

The concept of using KIDs to search for dark matter was proposed in 2008 [14]. Phonons are produced when the KID substrate reacts with dark matter. These phonons propagate to the KID and break its Cooper pairs. A recent proposal for a massive detector based on 108 individual 5 mm $\times$ 5 mm $\times$ 5 mm substrates, called BULLKID, aims to study dark matter and coherent elastic scattering of neutrinos [15].

We propose an alternative approach for the application of KIDs in astroparticle physics, particularly for rare event searches. Our approach involves the utilization of inorganic crystals as LEKID substrates. While silicon (Si), sapphire, and diamond are commonly used as KID substrates due to their accomplishments in semiconductor technology, our approach offers distinct advantages for using a diverse range of target crystals and enables easy scalability of the target mass by employing larger crystals with multiple readout. However, it should be noted that the appearance of LEKID resonances with inorganic crystal substrates cannot be guaranteed, nor can the detectability of substrate events be assured in phonon-mediated approaches. As the first step, our focus is on implementing LEKIDs on calcium fluoride (CaF_2) substrates. This choice is motivated by the prospects of dark matter searches utilizing spin-dependent interaction with ^{19}F, as well as studies of double beta decay in ^{48}Ca. In this paper, we present an experimental demonstration of the implementation of a LEKID on a CaF_2 substrate and a proof-of-concept of phonon-mediated particle detection on CaF_2 substrates.

2. Design and fabrication

The LEKID design consists of an inductive meander and interdigitated capacitor, as shown in Fig. 1. The SONNET simulation [16] predicts a resonant frequency of around 4.5 GHz for a Si substrate and 5.5 GHz for a CaF_2 substrate. The actual pattern is an array of 14 LEKIDs sharing a single feedline with different coupling distances ranging from 20 μm to 200 μm.

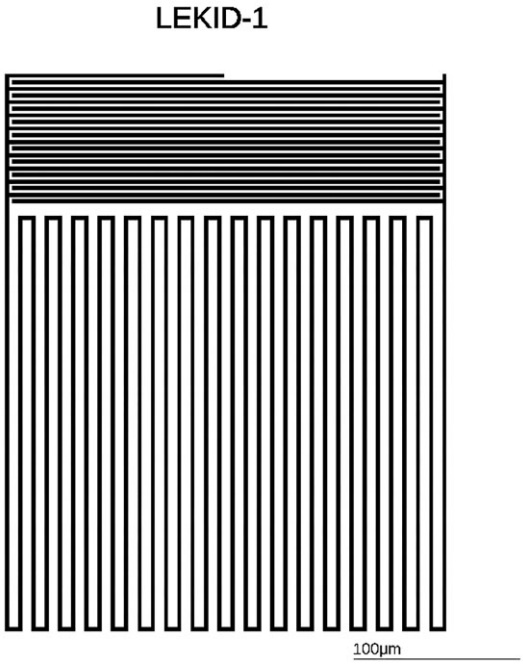

Fig. 1. Pattern of LEKID.

The LEKID elements were directly fabricated on a 10 mm × 10 mm CaF_2 substrate with a thickness of 1 mm at RIKEN. First, a 50 nm Al film was deposited on the substrate using a DC magnetron sputtering system. Then, a photoresist (Tokyo Ohka Kogyo Co., Ltd., TSMR 8900-LB) was coated onto the substrate. The photoresist was exposed by an LED at 50 mJ/cm^2 using a maskless exposure system (Nano System Solutions, Inc., DL-1000). After exposure, the designed pattern was developed using the developer (ROHM and Haas Electronic Materials Co., Ltd., MF-320). Finally, the Al film was removed by a wet etching process.

3. Evaluation

3.1. *Setup*

The LEKID was operated with a dilution refrigerator (Cryoconept, HEXA-DRY 200-UQT). The LEKID was placed in a permalloyed magnetic shield attached to a mixing chamber in the dilution refrigerator. We used CuNi coaxial cables to connect the outside of the refrigerator to the 4 K stage, and NbTi cables were used to link the 4 K stage to the mixing chamber.

For detailed studies, we employed a direct down-conversion (DDC) readout technique [17]. A field-programmable gate array (FPGA) on a Xilinx KCU705 was utilized to generate two digital waves, which were created by summing sinusoidal signals with a phase difference of $\pi/2$ at each resonant frequency. The digital waves were then converted into analog signals using RHEA [18]. These analog signals were up-converted using a radio frequency (RF) signal with a frequency of around 5 GHz from a local oscillator (LO) on an in-phase quadrature (IQ) mixer. The up-converted signals were then delivered to the LEKID through a DC block, attenuators, and a 4–6 GHz bandpass filter. The signal output from the LEKID was amplified using a high electron mobility transistor (HEMT) (Low Noise Factory, LNF-LNC-4_8A) on a 4 K stage and a room-temperature amplifier (Mini Circuits, ZVE-8G+). The amplified signal was then demodulated into in-phase (I) and quadrature-phase (Q) signals using an IQ demodulator with

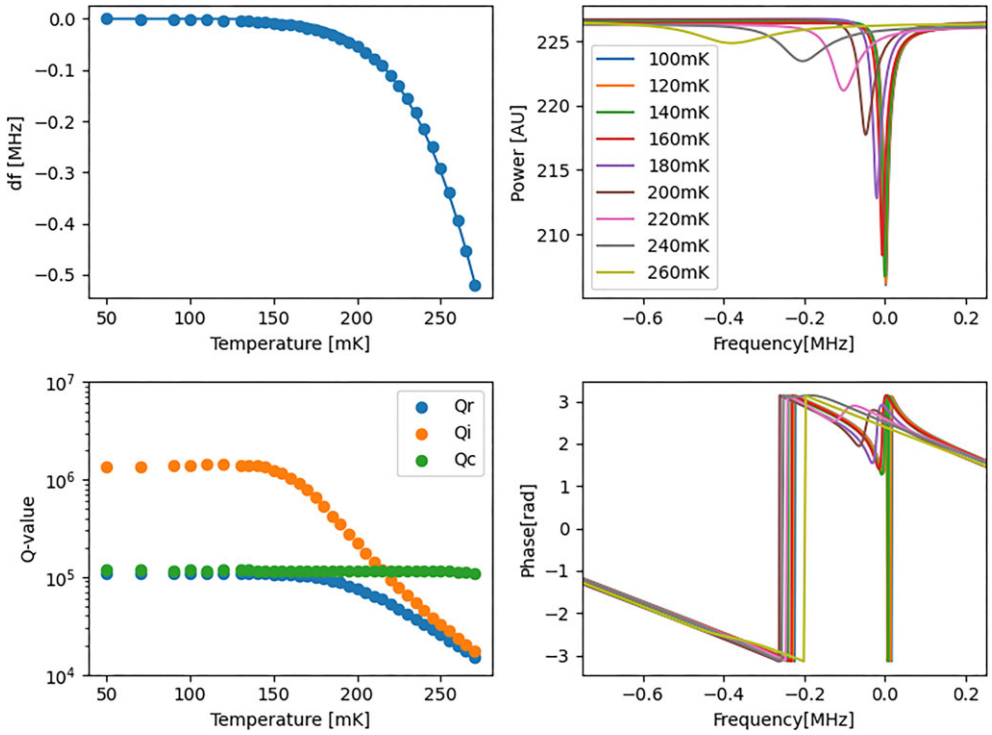

Fig. 2. The top left and bottom left panels show the resonance parameters as functions of the temperature. The fitted curves are also shown in the top left panel. The top right and bottom right panels show the changes in the resonance structure with temperature, where zero on the horizontal axis is the resonant frequency at the minimum temperature.

the same LO for up-conversion. These two demodulated signals were converted into two digital signals using the RHEA and sent to the FPGA. Finally, the FPGA utilized DDC logic to extract the time-ordered I and Q data for each LEKID resonant frequency.

3.2. *Resonance measurements*

The LEKID resonances were characterized by measuring their transmission $S_{21}(f)$ as a function of frequncy, f, which can be expressed as

$$S_{21}(f) = ae^{-2\pi i f \tau}\left[1 - \frac{Q_r/Q_c e^{i\phi}}{1 + 2iQ_r(f - f_0)/f_0}\right] = I(f) + iQ(f), \tag{1}$$

and fitted using a standard procedure [19]. Here Q_r, Q_i, and Q_c are a total quality factor of the resonator, internal quality factor, and coupling to the feedline, respectively. These are related to $1/Q_r = 1/Q_c + 1/Q_i$. a, τ, f_0, ϕ are the complex constant, cable delay, resonant frequency, and impedance mismatch, respectively.

From the measurements of $S_{21}(f)$, we confirmed that the six LEKIDs were active. The resonance parameters (Q_r, Q_c, Q_i, and f_0) were measured at various temperatures (T) and compared with the results obtained from LEKIDs on a silicon (Si) substrate. The measured f_0 ranged from 5.06 to 6.15 GHz/4.13 to 5.06 GHz when using the CaF_2/Si substrate. This difference is attributed to varying dielectric constants of the substrates, which is a phenomenon predicted by the SONNET simulation [16]. The resonance structure and parameters are shown for various T in Fig. 2. The measured values of Q_c exhibited no temperature dependence below 250 mK for either substrate. However, their magnitudes were distinct, with Q_c being (9–12) $\times$ 10^4 for

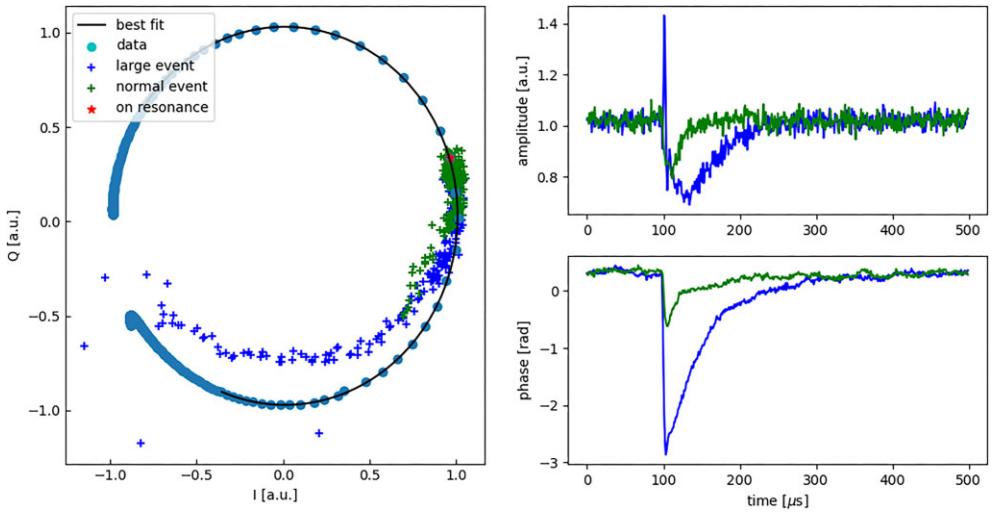

Fig. 3. The left panel shows the resonance in the $\mathcal{I}$-$\mathcal{Q}$ plane with the trigger TOD. The right panels are the amplitude and phase of the triggered TOD. We realize its large event and its normal event are an α-ray event and a γ-ray event, respectively.

the CaF_2 substrate and (2–6) $\times 10^4$ for the Si substrate. Conversely, the SONNET simulation displayed an opposite trend. Several LEKID elements were not assessed because of poor yields (approximately 50%) on the CaF_2 substrate, leading us to speculate that this difference arises from a reproducibility issue. Q_i remains constant below 150 mK. In contrast to Q_c, there is no significant disparity in Q_i values between the two substrates, with Q_i being (0.7–2.4) $\times 10^6$/(0.6–4.0) $\times 10^6$ for the CaF_2/Si substrate.

The change in resonant frequency can be expressed as follows [20],

$$\frac{f_0(T) - f_0^L}{f_0^L} = -\alpha \left[\tanh\left(\frac{\Delta_0}{2k_B T} \right)^{-1/2} - 1 \right], \tag{2}$$

where α and Δ_0 represent the fraction of the kinetic inductance relative to the total inductance and superconducting gap energy of the Al film, respectively. f_0^L is the resonant frequency at a temperature sufficiently below the superconducting transition temperature. Using the CaF_2 substrate, we obtained $\alpha = (7.4 \pm 0.4) \times 10^{-2}$ and $\Delta_0 = 155.8 \pm 1.6$ μeV. On the other hand, measurements conducted on Si substrates showed $\alpha = (3.6 \pm 0.3) \times 10^{-1}$ and $\Delta_0 = 208.8 \pm 0.8$ μeV. A notable difference was observed between the two results. It remains unclear whether this difference is due to the physical properties of the substrate or fabrication process. This will be investigated in future studies.

3.3. *Trigger measurements*

Hereafter, we focus on one single KID. We correct for the cable delay effect of $S_{21}(f)$ and transform the coordinates such that the origin is the center of the resonant circle, represented as $\mathcal{S}_{21}(f)$. The left panel of Fig. 3 shows an example of $\mathcal{S}_{21}(f)$ and its fitting curves based on Eq. (1) with the correction of the cable delay and coordinate transformation in the $\mathcal{I}$–$\mathcal{Q}$ plane, where $\mathcal{I} = \mathrm{Re}(\mathcal{S}_{21})$ and $\mathcal{Q} = \mathrm{Img}(\mathcal{S}_{21})$, respectively. Whenever $I(f_0)$ or $Q(f_0)$ exceeded the four-sigma thresholds previously measured, for four consecutive points, $I(f_0)$ and $Q(f_0)$ were recorded as time-ordered data (TOD) at 1 MS/s. Offline processing converts $I(f_0)$ and $Q(f_0)$ to $\mathcal{I}(f_0)$ and $\mathcal{Q}(f_0)$ as well as $S_{21}(f)$ to $\mathcal{S}_{21}(f)$. The phase $\theta = \arctan(\mathcal{Q}/\mathcal{I})$ is converted to

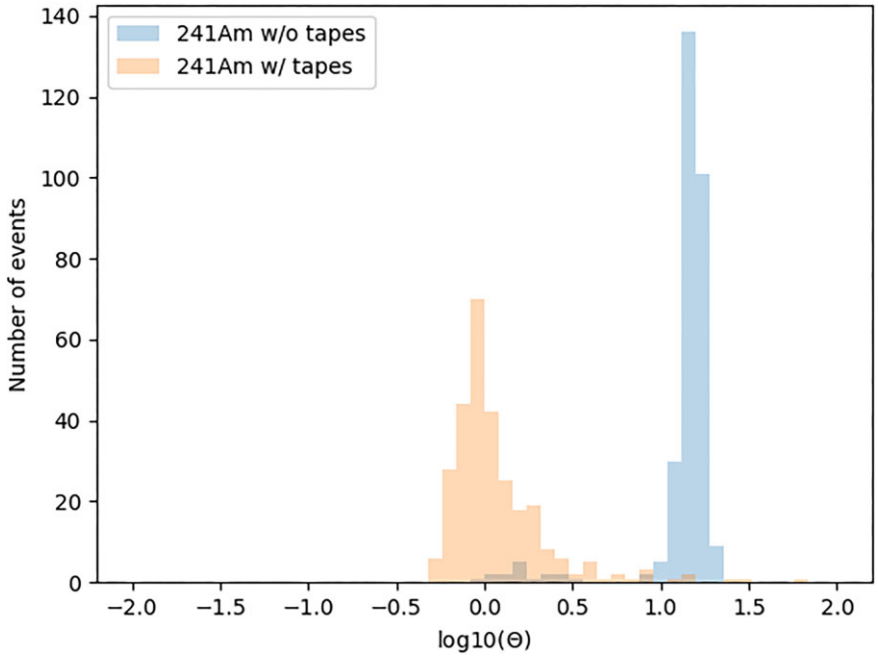

Fig. 4. Histograms of Θ when setting the ^{241}Am source with and without tapes.

$\Theta = 2\tan(\theta/2)$ for the nonlinear effect [21,22]. The distributions of the maximum phase Θ are shown in Fig. 4 attaching the ^{241}Am source with and without polyimide tapes. The ^{241}Am source emits 5.49 MeV α-rays and 59.5 keV γ-rays at approximately 110 Bq. The polyimide tapes are used to stop the 5.49 MeV α-rays. Thus, we can expect only γ-ray incidence with the tapes. Based on the geometric relationship, the trigger rate was considered to be approximately 10–20 Hz without the tapes. There is a clear peak around $\Theta = 15$ rad and the trigger rate is 13.3 $\pm$ 1.4 Hz. Without the source, the trigger rate is less than 30 mHz. The measured trigger rate is consistent with the expected value. Around $\Theta = 0.9$–1.5 rad, there is another small cluster. The other measurements with the tapes confirmed that they are 59.5 keV γ-ray events. The structure in the $\mathcal{I}$-$\mathcal{Q}$ plane and the change in amplitude ($\sqrt{\mathcal{I}^2 + \mathcal{Q}^2}$) and phase ($\theta$) without the correction are also shown in Fig. 3.

We confirmed that the LEKID on CaF_2 worked as a particle detector.

4. Discussion

In the ^{241}Am source run with the tapes, we observed a peak at $\Theta = 0.98$ rad (as shown in Fig. 4), which corresponds to a responsivity of $d\Theta/dE = 16.5$ mrad/keV. However, the 5.49 MeV α-rays yielded peaks around $\Theta \sim 15$ rad, leading to inconsistent results, even after applying the correction of $2\tan(\theta/2)$. The RMS noise level of the phase was determined to be 27 mrad through TOD analysis. Assuming a responsivity of 16.5 mrad/keV, the calculated five-sigma energy threshold is approximately 8.2 keV.

We can express the responsivity based on the number of quasiparticles in the superconducting film [21,23]. This expression relates the change in phase ($d\Theta$) to the deposited energy (dE) and can be given as:

$$\frac{d\Theta}{dE} = \eta \frac{\alpha S_2(f, T) Q_r}{N_0 V \Delta_0^2}, \tag{3}$$

where $N_0 = 1.72 \times 10^{10}$ eV$^{-1}\mu$m^{-3} represents the single-spin density of states, $S_2(f, T)$ is a temperature-dependent function of the resonant frequency characterizing the phase variation due to the breaking of Cooper pairs, $V = 1843.8$ μm^3 is the active volume of the resonator, and η is the efficiency from the energy deposit on the substrate to the breaking of Cooper pairs, respectively. Assuming $\eta = 0.01$ and $S_2(f, T) = 2.5$, we obtained a responsivity of $d\Theta/dE =$ 246 mrad/keV for one single KID, which is used in the trigger test. The variation of $S_2(f, T)$ with Al films appears to be relatively slow, ranging from 2.3 to 2.6 [24]. Assuming a responsivity of 246 mrad/keV, the resulting five-sigma energy threshold is approximately 550 eV. However, the parameter η carries a substantial level of uncertainty due to its dependency on several factors such as the mean free path of phonons in CaF_2.

The significant difference in responsivity between the incidence of 59.5 keV γ-rays and the analytical estimation based on the number of quasiparticles in the superconducting film raises several possibilities. One possibility is that the 59.5 keV energy is too strong to keep the linear relation. Another possibility is the overestimation of η. It is worth noting that even if 16.5 mrad/keV is confirmed, conducting combined amplitude and phase analysis as well as analyzing multiple KIDs simultaneously could help improve the situation [10,23].

This paper primarily emphasizes the demonstration of phonon-mediated particle detection through trigger rate analysis. For an energy-resolved particle detector, more assessments of responsivity and nonlinear response are required. However, these are beyond the scope of this paper. We intend to explore these aspects in a subsequent publication, where we will conduct measurements by irradiating the laser with varying laser power.

5. Summary

We proposed utilizing inorganic crystals on LEKID substrates in this paper. Cryogenic tests verified the resonance of a LEKID on the CaF_2 substrate and the capability of phonon-mediated particle detection. Therefore, the paper successfully demonstrated the proposed concept. The next phase of this study involves comprehensive performance evaluation for an energy-resolved particle detector using multiple LEKID elements. To further improve the energy threshold, we plan to develop a LEKID with an Al/Ti/Al trilayer structure or a single layer structure of hafnium (Hf), as demonstrated in previous studies (see examples of improvements with them in Refs. [25,26]).

Acknowledgements

This work was supported by Japan Society for the Promotion of Science (JSPS) KAKENHI Grant Numbers 19H05809, 19H01917, 21K18150, and 22K18708 and the US-Japan Science Technology Cooperation Program. The authors thank the GroundBIRD collaboration for providing the readouts. The authors thank the engineers at the Research Center for Neutrino Science, Tohoku University, who supported the cooling operation.

References

[1] R. Essig, G. K. Giovanetti, N. Kurinsky, D. McKinsey, K. Ramanathan, K. Stifter, and T.-T. Yu, Snowmass2021 Cosmic Frontier: The landscape of low-threshold dark matter direct detection in the next decade, in 2022 Snowmass Summer Study (2022), [arXiv:2203.08297 [hep-ph]] [Search INSPIRE].

[2] M. J. Dolinski, A. W. P. Poon, and W. Rodejohann, Ann. Rev. Nucl. Part. Sci. **69**, 219 (2019) [arXiv:1902.04097 [nucl-ex]] [Search INSPIRE].

[3] A. H. Abdelhameed et al., Phys. Rev. **D100**, 102002 (2019) [arXiv:1904.00498 [astro-ph.CO]] [Search INSPIRE].
[4] R. Agnese et al., Phys. Rev. Lett. **121**, 051301 (2018); **122**, 069901 (2019) [erratum][arXiv:1804.10697 [hep-ex]] [Search INSPIRE].
[5] V. Alenkov et al., Eur. Phys. J. **C79**, 791 (2019) [arXiv:1903.09483 [hep-ex]] [Search INSPIRE].
[6] Y. Hochberg, I. Charaev, S.-W. Nam, V. Verma, M. Colangelo, and K. K. Berggren, Phys. Rev. Lett. **123**, 151802 (2019) [arXiv:1903.05101 [hep-ph]] [Search INSPIRE].
[7] A. Vayonakis, P. K. Day, H. G. LeDuc, B. A. Mazin, and J. Zmuidzinas, Nat. **425**, 817 (2003).
[8] S. Doyle, P. Mauskopf, J. Naylon, A. Porch, and C. Duncombe, J. Low. Temp. Phys. **151**, 530 (2008).
[9] L. J. Swenson, A. Cruciani, A. Benoit, M. Roesch, C. S. Yung, A. Bideaud, and A. Monfardini, Appl. Phys. Lett. **96**, 263511 (2010) [arXiv:1004.5066 [physics.ins-det]] [Search INSPIRE].
[10] D. C. Moore, S. R. Golwala, B. Bumble, B. Cornell, P. K. Day, H. G. LeDuc, and J. Zmuidzinas, Appl. Phys. Lett. **100**, 232601 (2012) [arXiv:1203.4549 [astro-ph.IM]] [Search INSPIRE].
[11] E. S. Battistelli et al., Eur. Phys. J. **C75**, 353 (2015) [arXiv:1505.01318 [physics.ins-det]] [Search INSPIRE].
[12] L. Cardani, N. Casali, I. Colantoni, A. Cruciani, S. Di Domizio, M. Martinez, V. Pettinacci, G. Pettinari, and M. Vignati, Eur. Phys. J. C, **81**, 636 (2021) [arXiv:2104.06850 [physics.ins-det]] [Search INSPIRE].
[13] N. Casali, L. Cardani, I. Colantoni, A. Cruciani, S. Di Domizio, M. Martinez, G. Pettinari, and M. Vignati, Eur. Phys. J. **C79**, 724 (2019) [arXiv:1907.03647 [physics.ins-det]] [Search INSPIRE].
[14] S. Golwala, J. Gao, D. Moore, B. Mazin, M. Eckart, B. Bumble, P. Day, H. G. LeDuc, and J. Zmuidzinas, J. Low. Temp. Phys. **151**, 550 (2008).
[15] A. Cruciani et al., Appl. Phys. Lett. **121**, 213504 (2022) [arXiv:2209.14806 [physics.ins-det]] [Search INSPIRE].
[16] SONNET software, 2023. https://www.sonnetsoftware.com.
[17] O. Bourrion, C. Vescovi, J. L. Bouly, A. Benoit, M. Calvo, L. Gallin-Martel, J. F. Macias-Perez, and A. Monfardini, J. Instrum. **7**, P07014 (2012).
[18] H. Ishitsuka, M. Ikeno, S. Oguri, O. Tajima, N. Tomita, and T. Uchida, J. Low. Temp. Phys. **184**, 424 (2016).
[19] S. Probst, F. B. Song, P. A. Bushev, A. V. Ustinov, and M. Weides, Rev. Sci. Instrum. **86**, 024706 (2015) [arXiv:1410.3365 [cond-mat.supr-con]] [Search INSPIRE].
[20] P. Diener, H. Schellevis, and J. J. A. Baselmans, Appl. Phys. Lett. **101**, 252601 (2012).
[21] J. Gao, The physics of superconducting microwave resonators, PhD thesis, California Institute of Technology (2008).
[22] H. Kutsuma, M. Hattori, R. Koyano, S. Mima, S. Oguri, C. Otani, T. Taino, and O. Tajima, Appl. Phys. Lett. **115**, 032603 (2019) [arXiv:1907.03403 [astro-ph.IM]] [Search INSPIRE].
[23] L. Cardani et al., Appl. Phys. Lett. **110**, 033504 (2017) [arXiv:1606.04565 [physics.ins-det]] [Search INSPIRE].
[24] L. Cardani et al., Appl. Phys. Lett. **107**, 093508 (2015) [arXiv:1505.04666 [physics.ins-det]] [Search INSPIRE].
[25] L. Cardani et al., Supercond. Sci. Technol. **31**, 075002 (2018) [arXiv:1801.08403 [physics.ins-det]] [Search INSPIRE].
[26] N. Zobrist et al., Appl. Phys. Lett. **115**, 213503 (2019) [arXiv:1911.06434 [astro-ph.IM]] [Search INSPIRE].